

## Enhancement of Oxygen Transfer in Hollow Fiber Membrane by the Vibration Method

Gi-Beum Kim<sup>†</sup>, Seong-Jong Kim<sup>\*</sup>, Chul-Un Hong, Tae-Kyu Kwon and Nam-Gyun Kim

Division of Bionics and Bioinformatics, College of Engineering, Chonbuk National University,  
664-14 1ga, Duckjin-dong, Duckjin-gu, Jeonju 561-756, Korea

<sup>\*</sup>Dept. of Applied Materials Engineering, Iksan National College, 194-5, Ma-dong, Iksan 570-752, Korea

(Received 17 January 2005 • accepted 12 May 2005)

**Abstract**—The purpose of this study was to assess and quantify the beneficial effects of gas exchange according to the various frequencies of the sinusoidal wave that are excited by a PZT actuator, on patients suffering from acute respiratory distress syndrome (ARDS). In this study, an experimental method for the flow hydrodynamics was developed through a bundle of sinusoidally vibrated hollow fibers to observe how well vibrations might enhance the performance of the VIVLAD. We measured the effect of the various excitation frequencies of the PZT actuator on the gas transfer rates and hemolysis from the maximum gas transfer rate. As a result, the maximum oxygen transfer rate was reached at the maximum amplitude and through the transfer of vibrations to the hollow fiber membranes. The device was maximum excited by a frequency band of 7 Hz at various water flow rates, as this frequency was the 2nd mode resonance frequency of the flexible beam. 675 hollow fiber membranes were also bundled, within the blood flow, into the device.

Key words: Artificial Lung, Gas Transfer, Hollow Fiber Membranes, Vibration, Hemolysis

### INTRODUCTION

Acute respiratory distress syndrome (ARDS) is a form of acute respiratory failure caused by an extensive lung injury after a variety of catastrophic events such as shock, severe infection, and burns. ARDS can occur in individuals with or without previous lung disease, through exposure to noxious gases, steam, or heat during a fire, which can result in respiratory failure. Respiratory failure usually occurs following a catastrophic event in individuals with no previous lung disease. Regardless of the event causing the lung injury, the patients exhibit common signs and symptoms, x-ray findings, and tissue changes. Because many of its features resemble the type of respiratory distress syndrome of newborns, ARDS, the adult disease is also called ARDS.

The disease affects approximately 150,000 people per year in the United States [Fazzalari et al., 1994] and treatment requires respiratory support using the conventional therapy of mechanical ventilation, or extracorporeal membrane oxygenation (ECMO) for patients with severe ARDS. The positive airway pressures and volume excursions associated with mechanical ventilation can cause further damage to the lung tissue, including barotrauma, volutrauma and parenchyma damage from the toxic levels of oxygen needed for effective mechanical ventilation [Weinberger et al., 1992]. The alternative use of ECMO is complicated and expensive, requiring extensive blood/biomaterial contact in extracorporeal circuits, systemic anticoagulation, and labor-intensive patient monitoring. Due to these complications, the mortality rate of ARDS patients is very high, exceeding 50% in adults [Gattinoni et al., 1980; Pesenti et al., 1988; Snider et al., 1988; Campell et al., 1994; Ichiba et al., 1996; Fedespiel et al., 1997; Hewitt et al., 1998].

Intravascular oxygenation represents an attractive, alternative sup-

port modality for patients with ARDS. The concept of intravascular oxygenation as an alternative ARDS therapy was first reported by Mortensen [Mortensen et al., 1992], who developed an intravenous oxygenator (IVOX) consisting of a bundle of crimped hollow fibers positioned in the vena cava. In clinical trials, the IVOX provided an average of 28% of the basal gas exchange requirements for patients with severe ARDS [Conrad et al., 1994]. However, clinical studies concluded that more gas exchange is needed for intravascular oxygenation to be effective in ARDS treatment.

We are in the process of developing an intravenous membrane oxygenator with a design goal of 50% of the base oxygen and carbon dioxide exchange requirements for end-stage ARDS patients [Lee and Kim 2002; Kim et al., 2003]. Like the IVOX, the intravenous membrane oxygenator consists of a bundle of manifolded hollow fibers, and is intended for the intravenous placement within the superior and inferior vena cava. Consequently, the intravenous membrane oxygenator incorporates a vibrating actuator concentric with the fiber bundle, which enhances gas exchange. Currently, efforts are focused on the device improvements intended to provide the target levels of gas exchange, given the constraints imposed by the intravenous placement on fiber bundle size and hence the fiber area for gas exchange. Although critical care techniques have improved, the high mortality of severe acute respiratory failure (ARDS) has not changed significantly [Woodhead et al., 1992; Nguyen et al., 1993]. In an intravenous membrane oxygenator, the greater part of the oxygen transfer resistance is located in the blood-side of the laminar film [Vaslef et al., 1994]. Various methods to improve the laminar film in order to improve the oxygen transfer rate have been attempted [Weissman et al., 1968; Tanishita et al., 1975].

This study developed an analytical solution for the hydrodynamics of flow through a bundle of sinusoidally vibrated hollow fibers, which is used to provide some insight into how wall vibrations might enhance the performance of an intravascular lung assist device. Scaling analysis was then used to determine the dimensionless groups

<sup>†</sup>To whom correspondence should be addressed.

E-mail: kgb70@chonbuk.ac.kr

that correlate the performance of a vibrated hollow tube membrane oxygenator. The experimental design and procedure for a device given were then used to assess the effectiveness of membrane vibrations. The aim of this study was to assess and determine if the beneficial effects in the long-term gas exchange at a fixed excited frequency could be obtained at the different frequencies, and then to develop an intravascular lung assist device (IVLAD) for patients having chronic respiratory problems.

## THEORY

### 1. Description of Mass Transfer

For the Reynolds numbers, the dimensionless rate of mass transfer,  $K$ , is given by

$$K = N_{Sh} N_{Sc}^{-1/3} = \alpha N_{Re}^{\beta} \quad (1)$$

The Reynolds number,  $N_{Re}(=dv/\nu)$ , characterizes the flow regime and is the ratio of the inertial force to the viscous force. The Schmidt number,  $N_{Sc}(=\nu/D)$ , which is analogous to the Prandtl number in heat transfer, characterizes the fluid properties and is the ratio of the momentum transport to diffusive transport. The Peclet number,  $N_{Pe}(=dv/D)$ , which is the product of  $N_{Re}$  and  $N_{Sc}$ , characterizes the relative importance of the convective and diffusive processes, and is the ratio of bulk mass transport to diffusive mass transport. The Sherwood number,  $N_{Sh}(=Kd/D)$ , which is also known as the mass transfer Nusselt number, likewise characterizes the relative importance of convective and diffusive transport, and it is the ratio of the total transport to diffusive transport. In which  $d$  is the characteristic length,  $\nu$  is the velocity,  $D$  is the diffusivity,  $\nu$  is the kinematic viscosity and  $K$  is the mass transfer rate [Streeter et al., 1998; Bird et al., 2002; Mulder, 1996; Beek et al., 1996].

The characteristic length is given by

$$d = \frac{\varepsilon}{1 - \varepsilon} d_o \quad (2)$$

where  $\varepsilon$  is the device porosity, and  $d_o$  is the outside diameter of the hollow fiber membrane.

The  $O_2$  content and  $O_2$  transfer rate were calculated by the following standard formulae:

$$O_2 \text{ content (vol\%)} = \frac{Hb \times 1.34 \times \% O_2 \text{ saturation}}{100} \times P_{O_2} \times 0.003 \quad (3)$$

$$O_2 \text{ transfer rate (ml/min)} = (C_{aO_2} - C_{vO_2}) \times \text{blood flow rate} \quad (4)$$

where  $Hb$  is the hemoglobin level (g/ml),  $P_{O_2}$  is the partial pressure of oxygen (mmHg), 1.34 being the amount (in ml) of oxygen that could be carried by 1 g of hemoglobin; and 0.003 is the amount (in ml) of oxygen that can be dissolved for each 1 mmHg.  $C_{aO_2}$  is the arterial oxygen content (vol%),  $C_{vO_2}$  is the venous oxygen content (vol%), and the blood flow rate represents the pump flow rate (l/min).

### 2. Calculation of Normalized Index of Hemolysis

Blood hemolysis is expressed as the Normalized Index of Hemolysis (NIH) according to this equation [Snider et al., 1972; Morin et al., 1977; Naito et al., 1994; Nosè et al., 1998]:

$$NIH(\text{g}/100\text{L}) = \frac{\Delta fHb \times V \times \left(1 - \frac{Ht}{100}\right) \times 100}{\Delta t \times Q} \quad (5)$$

**Table 1. Inlet parameters recommended by AAMI/ASTM Standard: Admitted range, minimum and maximum values measured during the test**

	AAMI Recommended range	Measured		
		Average	Min.	Max.
T (°C)	37±1	37.0	36.8	37.2
B.E. (mmol/l)	0±5	1.1	-1.8	2.7
SvO2 (%)	65±5	65.5	64.0	68.0
Hb (g/ml)	12±1	12.0	11.6	12.5

where,  $\Delta fHb$  is the increase in the free plasma hemoglobin concentration during the testing time,  $Ht$  is the percentage of hematocrit,  $V$  is the blood volume for each circuit, and  $Q$  is the flow rate expressed in l/min.

## MATERIALS AND METHODS

### 1. Blood Condition

The blood was obtained from cattle with a normal body temperature, no physical signs of disease, including diarrhea or rhinorrhea, and an acceptable range of hematological profiles. The blood was collected by a vascular puncture using a needle (14G) and placed into 500 ml blood bags, which contained a citrate phosphate dextrose adenine (CPDA-1) anticoagulant solution. Table 1 shows that the initial mean free hemoglobin concentration was  $5.33 \pm 2.75$  mg/ml, and the mean hematocrit was  $28.1 \pm 3.0\%$ . All of the units of blood were used within 6 hours of acquisition.

### 2. Membrane Oxygenator

In this study, the experimental data was measured to evaluate the performance of the Vibrating Intravascular Lung Assist Device (VIVLAD). The test section was a cylinder duct with an axial length of 60 mm, and an inner diameter of 30 mm. Fig. 1 shows a photograph of the VIVLAD. The VIVLAD used for this experiment was prepared by using the number of hollow fibers in the acrylic cylinder, as shown in Fig. 2. The VIVLAD was made from micro porous polypropylene with an inner diameter of 380  $\mu\text{m}$  and a membrane thickness of 50  $\mu\text{m}$  (Oxyphane, Enka, Germany), respectively. The experimental set-up of a flexible beam in the artificial lung device is shown in Fig. 2. The material used for the tests is a random glass fiber reinforced polypropylene composite. The thickness of the sheet was 1 mm for 40% glass sheet. The PVDF was LDT1-028K (AMP, 28  $\mu\text{m}$  thickness). The piezoceramic used is a multi-layer bender PZT actuator which is PL-128.255 Lead Zirconate Titanate (PZT) of Digital ECHO company. The dimension is  $40 \times 10 \times 0.45$  mm. The

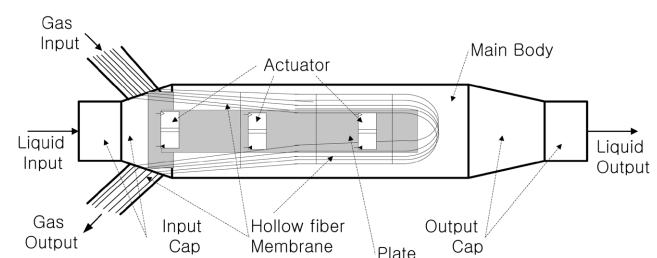


**Fig. 1. Vibrating intravenous lung assist device (VIVLAD).**

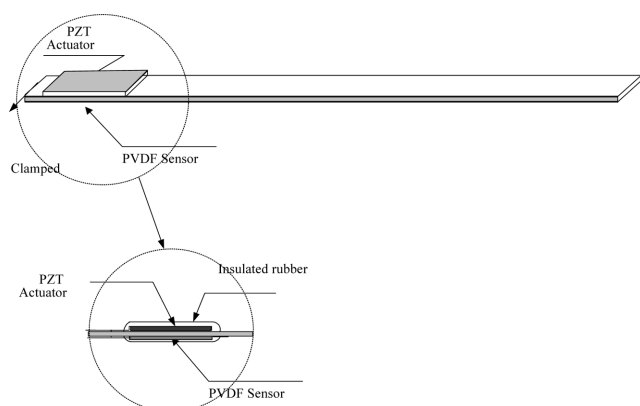


**Fig. 2. Configuration of a cantilevered composite beam with the piezo-film sensor and piezo-ceramic actuator.**

PZT and PVDF were bonded to the beam with araldite adhesive, and the electrical leads were soldered to the electrode of piezo-elements, and then covered by elastic rubber for waterproofing. The PZT actuator and PVDF sensor were bonded to a flexible beam with Araldite®, and the electrical leads were soldered to the electrode of the piezo-elements. Elastic rubber was then used to waterproof the electrical leads. A description of the VIVLAD is given in Table 2.

### 3. Test Circuit

Fig. 3 shows the experimental closed loop for the gas performance tests. The experimental closed loop blood circuit consisted of a bio-compatibility tube with an inner diameter of 3/8 inch, the deoxygenator (Baxter Healthcare Corporation, Irvine, CA, USA), the electromagnetic blood flow meter, a roller pump (Cobe Cardiovascular, Inc., Arvada, Co. USA), and a membrane oxygenator. A gas blender (Sechrist Industries, Inc., Anaheim, CA) was connected to the deoxygenator with tubing. The blood temperature was maintained at 37 °C with a heat exchanger.

### 4. Measurements

The measurement was performed according to the AAMI/ISO international standard recommendations [AAMI, 1998; ISO/DIS, 1996]. The experimental closed loop was primed to less than 6 liters of filtered cattle blood after the addition of 75 ml ADC and 1 ml heparin for anticoagulation. The hemoglobin content was calibrated at the required value ( $12.0 \pm 1.0$  g/ml) by means of a blood dilution with normal saline. Adequate recirculation was performed prior to the test, in order to adjust the blood's inlet conditions according to the AAMI/ISO standards (Table 1). The total duration of the test was 6 hours. The mean blood flow rate ( $Q_b=6.0$  l/min or smaller and the systolic period of the vibration waveform (50% of the entire cycle) were constant. Gas flow rates of up to 6 l/min through the

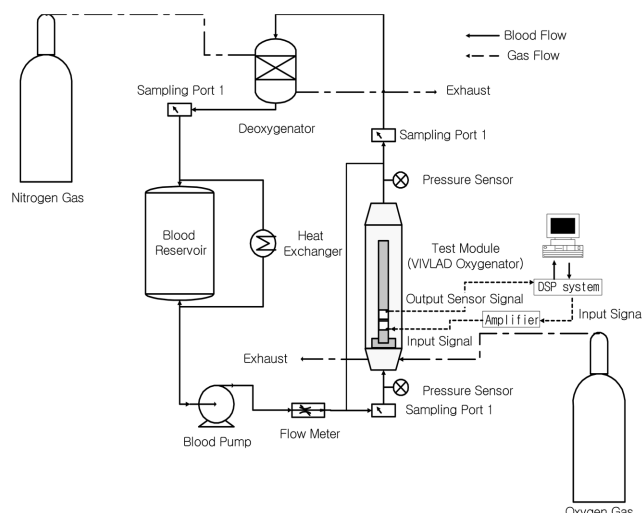


**Fig. 3. In vitro bench test system used for the oxygen transfer and of the test modules.**

120-cm-long hollow fibers were achieved by exciting a piezo vibrator with a sinusoidal wave magnitude of DC 50 V.

Fig. 3 shows the experimental setup of the testing equipment for measuring the level of blood oxygen transfer. The experiment was carried out using a DSP 1104 board (TMS320C40, dSPACE GmbH, Germany) and an amplifier (SQV 3/150, Pizomechanik Dr. L. Piekeman GmbH, Germany). The signal from an A/D converter with a sampling ratio of 1 ms was sent to the DSP system and the calculated input voltage was sent to a PZT actuator to excite the test module through the D/A converter and amplifier.

The signals from the sensor according to the applied input voltage were digitalized and filtered in order to obtain the dynamic characteristics of the flexible beam in the artificial lung device. In the filtering procedure, the DC offset was rejected and the noise was eliminated with a cutoff frequency of 0.5 Hz and 50 Hz using a band-pass filter (BPF), respectively. Finally, the signals were integrated in order to measure the applied input voltage. The processed signals of the sensor output were obtained from a personal computer while the experiment was underway.

The experiments were performed at various frequencies that are applied to the PZT actuator of the test module. The dynamic response of the sensor system was obtained by applying the dynamic input voltage with the frequencies of the sinusoidal wave ranging from 0 Hz to 50 Hz, the magnitude of the excited input ranged from 0 to 100 V. The measuring system was discretized at every sampling interval of 0.001 s. Every hour, the excitation frequency of the test module ranged from 0 to 10 Hz (step 1 Hz) in four runs lasting for 60 minutes each. Under each run, three veno/arterial blood samples

**Table 2. Dimensions of hollow fiber modules**

Parameter	Type 1	Type 2	Type 3	Type 4	Type 5
Membrane type	Hollow fiber	Hollow fiber	Hollow fiber	Hollow fiber	Hollow fiber
Material	Polypropylene	Polypropylene	Polypropylene	Polypropylene	Polypropylene
Cylinder duct inner diameter (mm)	30	30	30	30	30
Number of hollow fiber	100	200	300	450	675

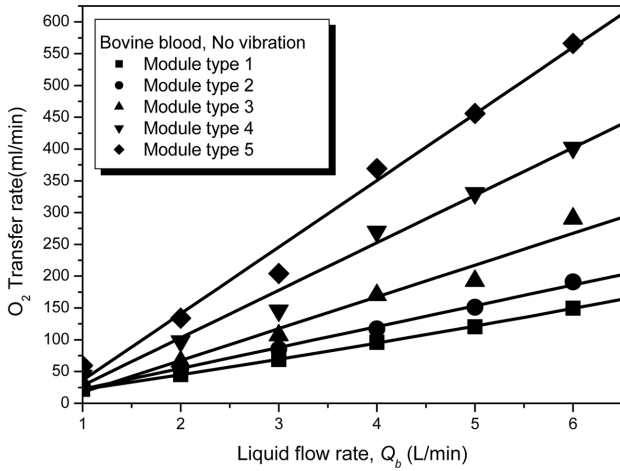
were withdrawn and analyzed immediately. The flow rate of oxygen was matched with the flow rate of blood. The samples were taken from the inlet and outlet sampling ports, and the blood gases were analyzed by using an i-Stat Portable Blood Gas/Electrolyte Analyzer (i-Stat Co., East Windsor, NJ, USA). Data collection consisted of recording the venous and arterial oxygen saturation values

( $Sv_{O_2}$ ,  $Sa_{O_2}$ ), the oxygen partial pressure ( $pv_{O_2}$ ,  $pa_{O_2}$ ), the venous and arterial pH, and the total concentration of hemoglobin (Hb) in the exhausted gas.

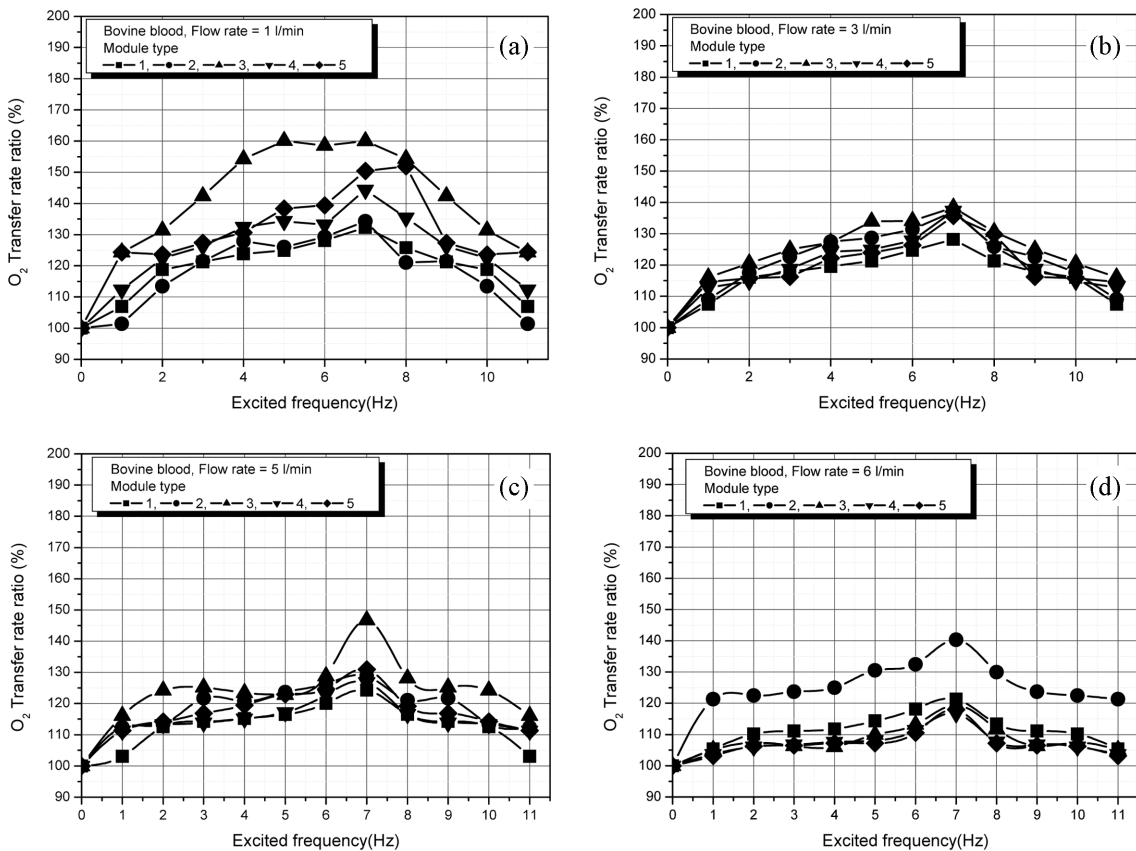
**RESULT AND DISCUSSIONS**

Fig. 4 shows the relationships between the oxygen transfer rate and various flow rates without an excited vibration. When the blood flow rate was increased, the oxygen transfers rate increased, and the module type 5 shows a higher oxygen transfer rate than any of the other types. Module type 5 consisted of 675 hollow fiber membranes. The membrane module consisting of up to 675 hollow fibers of type 5 was observed having a pressure drop of 14.6 mmHg at the flow rate speed of 6 l/min, which can satisfy the condition where the blood pressure drop must be maintained below 15 mmHg in order to apply the VIVLAD the vein. Good agreement between the hypothesis and experiment results at 6 l/min was also shown.

Fig. 5 shows the relationships between the excited frequency and the oxygen transfer rate on blood flow rate at various module types. The maximum oxygen transfer rate appeared to be caused by the occurrence of a maximum amplitude and transfer of the vibration to the hollow fiber when it was excited by 7 Hz at each blood flow rate. This is because this frequency became the 2nd mode resonance frequency of the flexible beam inserted into the VIVLAD. The excited frequency region for the maximum oxygen transfer rate at DC50V was approximately 7 Hz. When it was excited at



**Fig. 4. Relation between the flow rate of bovine blood and oxygen transfer rate on the various number of hollow fibers in bovine blood at 37°C.**



**Fig. 5. Oxygen transfer rate for VIVLAD, of various module types, and liquid flow rate, using bovine blood at various excited frequencies (Blood flow rate (a) 1 l/min, (b) 3 l/min, (c) 5 l/min, (d) 6 l/min).**

more than 8 Hz, the oxygen transfer rate was relatively lower than it was at 7 Hz. The oxygen transfer rate also increased in each excited frequency bandwidth compared to the rate without the vibration. There was little difference among the oxygen transfer rates regardless of the vibration when the blood flow rate was relatively low, for example at 1 l/min. However, the increase in the blood flow rate affected the oxygen transfer rate significantly. There was a large resonance affecting the oxygen transfer rate at a high blood flow rate, 6 l/min, because there was a large resonance between the excitation frequency of the flexible beam and the blood flow rate at

the excitation frequency of 7 Hz. The resonance effect indicates the doubled effects as a result of the coupling of the excitation frequency of the test module and the blood flow. However, initially, the array of the effective hollow fiber membrane was quite important because the effect of the oxygen transfer changed according to the contact states between the hollow fiber membrane and blood.

Fig. 6 shows the output voltage of the PVDF sensor at the maximum oxygen transfer rate in module type 4. As shown in this figure, the maximum amplitude of the PVDF sensor output was at the frequency band of 7 Hz in various blood flow rates. The maximum oxygen transfer effect occurred at the frequency band of 7 Hz. This resonance effect represented the maximum oxygen transfer rate by reducing the boundary layer, which occurred on the surface of the hollow fiber membrane.

Fig. 7 shows the dependence of the mass transfer rate,  $K$ , of the blood flow in the VIVLAD at the various excited vibrations. The mass transfer rate increased with the linear velocity of the blood flow. A lower number of tied hollow fibers produce a higher mass transfer rate at a constant velocity of the blood-side flow. These results indicate that the packing of the hollow fiber strongly affects the mass transfer rate. This figure is a log-log plot of  $K$  vs.  $N_{Re}$  for the VIVLAD experiment at various numbers of tied hollow fibers. The following equations were obtained by the least-square fits method.

$$K = \alpha N_{Re}^{\beta}$$

$$\alpha = y_0 + A e^{-f t}$$

$$y_0 = 0.52 + 58.47 e^{-f^{0.03}}$$

$$A = -0.07 - 5.47 e^{-f^{0.04}}$$

$$t = 2.48 + 0.0001 e^{-f^{0.22}} \tag{6}$$

$$\beta = A' + B' x$$

$$A' = 0.98 - 0.31 e^{-p^{0.02}}$$

$$B' = 0.004 - 0.012 p^* \tag{7}$$

These values for the slope and vertical position were used in the equation,  $K = \alpha N_{Re}^{\beta}$ , to predict  $O_2$  transfer rates in distilled water for the VIVLAD at the various numbers of tied hollow fibers.

Fig. 8 shows the relationship between the changes in the plasma free hemoglobin and time at different flow rates in module type 5, indicating the maximum oxygen transfer rate. Fig. 8 shows the changes in the plasma free hemoglobin with each PZT actuator activated with sinusoidal wave amplitude of DC10V. The change in the plasma free hemoglobin was 0.112 g/ml after 6 hours with sinusoidal wave amplitude of DC10V and an excitation frequency band of 7 Hz at the blood flow rate of 5 l/min in module type 5. From the results of blood hemolysis, it was determined that damage to the blood does not occur because the hemolysis is low, which was measured during the 6 hours of excitation in frequency region of 7 Hz in the experiment. Enhancing the performance of the contactors using the membrane vibrations also offers an additional advantage of minimizing fouling. Employing membrane vibrations may be more amenable to enhancing the performance of an implantable blood oxygenator because it is easier to implement and is less traumatic than when employing direct pulsations of the fluid flow.

### CONCLUSION

The hemolysis was low in the frequency band of 7 Hz, which

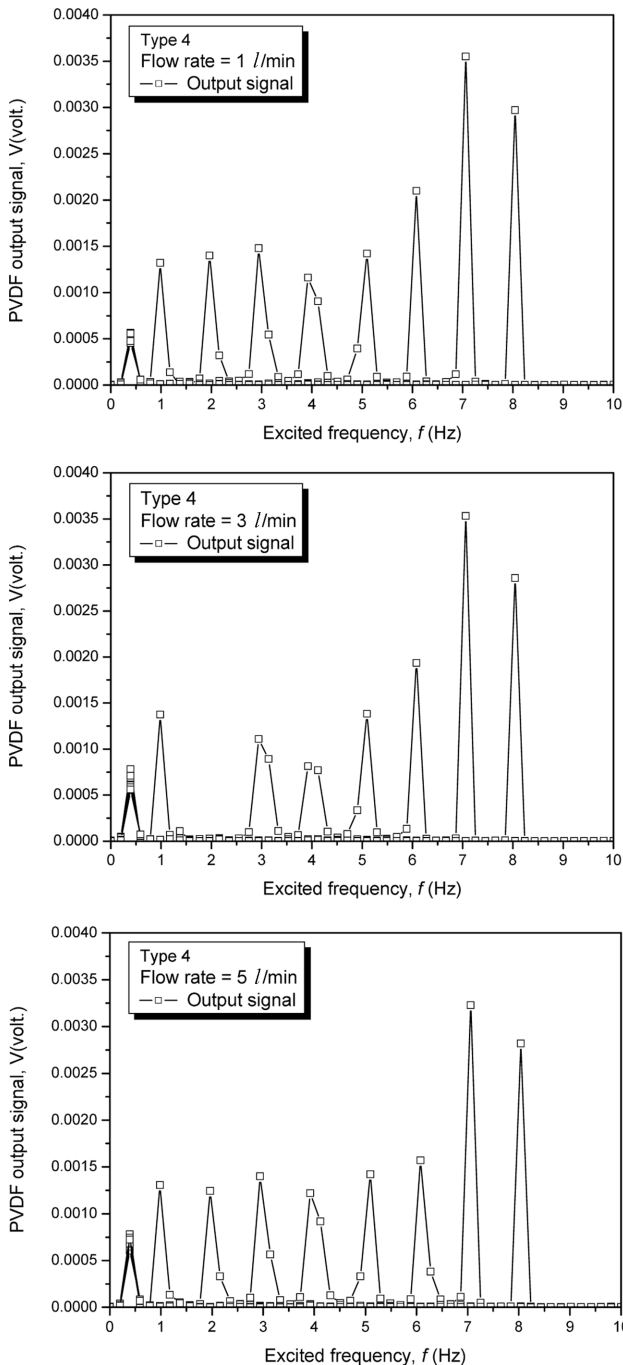


Fig. 6. Amplitude of PVDF sensor output the system for various excited frequencies with bovine blood.

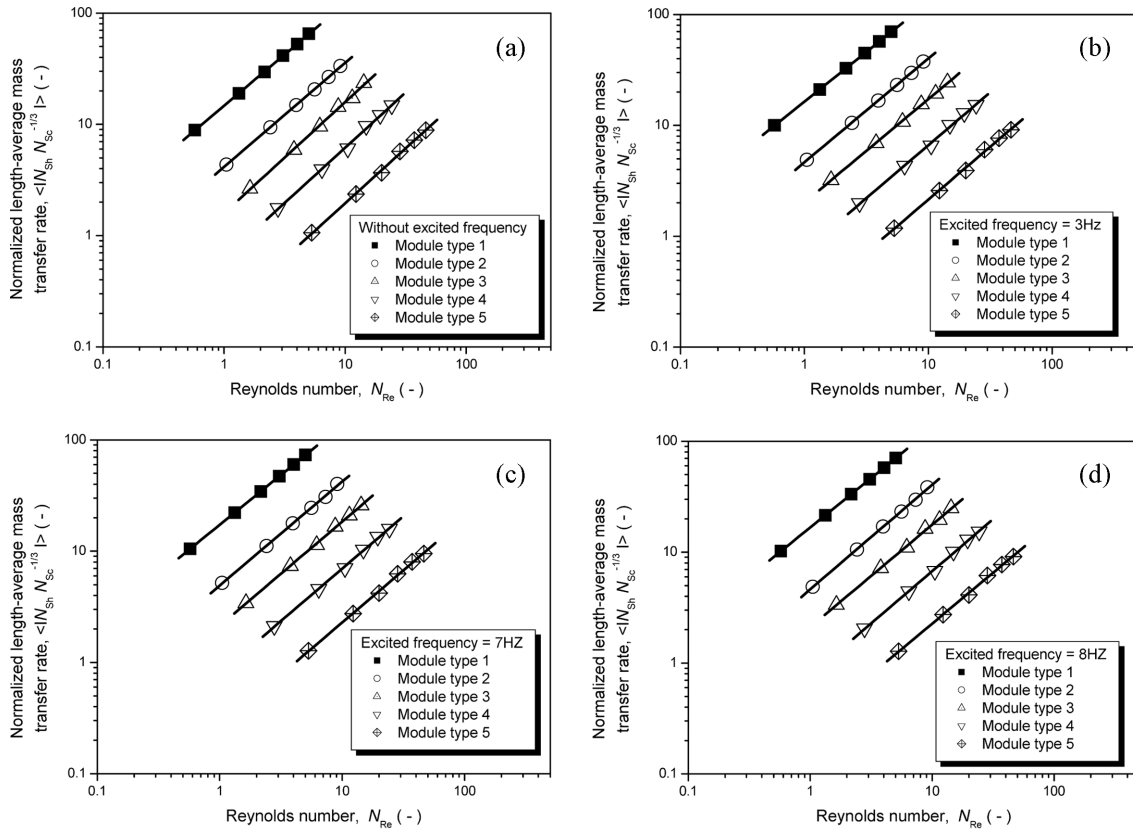


Fig. 7. Oxygenation performance of VIVLAD of various module types using bovine blood at various excited frequencies (Excited frequency (a) without excited, (b) 3 Hz, (c) 7 Hz, (d) 8 Hz).

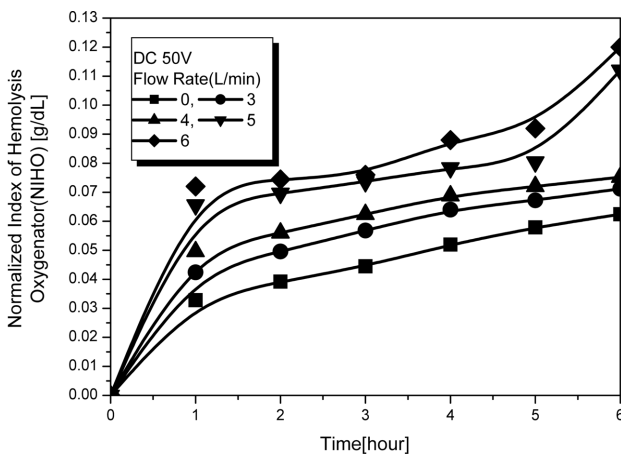


Fig. 8. Graph reveals a variety in plasma free hemoglobin as various blood flow rate with the passage of time excited at 7 Hz.

had a maximum value for the oxygen transfer rate. It is known that the resonance frequency band of 7 Hz in the blood experiments has a maximum oxygen transfer rate. In addition, the hemolysis in the module was judged to be able to improve the oxygen velocity efficiency by not adversely affecting blood by the 7 Hz area because the hemolysis was low at the time when the new device was excited at the frequency band of 7 Hz for 6 hours. As a result, the effect of the various exciting frequencies in gas transfer rates and hemolysis could be measured by using the maximum gas transfer rate. The

maximum oxygen transfer rate was reached through the occurrence of the maximum amplitude, and the transfer of a vibration to the hollow fiber membranes. This is because this frequency was the 2nd mode resonance frequency of the flexible beam, which was also bundled with 675 hollow fiber membranes in the blood flow. In addition, the blood hemolysis was low when module type 5 was excited at a frequency band of 7 Hz. Therefore, it was determined that the limit of the hemolysis frequency was the frequency band of 7 Hz, because the maximum amplitude was obtained from the PVDF sensor at this frequency.

ACKNOWLEDGMENTS

This research was supported by the Korean Ministry of Education & Human Resources Development through the Center for Healthcare Technology Development.

REFERENCES

AAMI Standard: Cardiovascular/Neurology Standards for Blood/Gas Exchanger Devices (Oxygenators); August 14 (1998).  
 Beek, W. L., Muttzell, K. M. K. and van Heuven, J. W., *Transport Phenomena* (2th ed.), John Wiley & Sons (ASIA) PTE LTD, Singapore, 262 (1999).  
 Bird, R. B., Stewart, W. E. and Lightfoot, E. N., *Transport Phenomena* (2th ed.), New York, John Wiley & Sons Inc., 675 (2002).  
 Campell, T. G., "Changing Criteria for the Artificial Lung: Historic Con-

- trols on the Technology of ECMO," *ASAIO J.*, **40**, 109 (1994).
- Conrad, S. A., "Major Findings from the Clinical Trials of the Intravascular Oxygenator," *Artificial Organs*, **18**, 846 (1994).
- Fazzalari, F. L., Bartlett, R. H., Bonnel, M. R. and Montoya, J. P., "An Intrapleural Lung Prosthesis: Rationale, Design and Testing," *Artificial Organs*, **18**, 801 (1994).
- Fedespiel, W. J., Hout, M. S., Hewitt, T. J., Lund, L. W., Heinrich, S. A., Litwak, P., Walters, F. R., Reeder, G. D., Borovetz, H. S. and Hattler, B. G., "Development of a Low Flow Resistance Intravenous Oxygenator," *ASAIO J.*, **43**, M725 (1997).
- Gattinoni, L., Pesenti, A. and Rossi, G. P., "Treatment of Acute Respiratory Failure with Low-frequency Positive-pressure Ventilation and Extracorporeal Removal of CO<sub>2</sub>," *Lancet*, **2**, 292 (1980).
- Hewitt, T. J., Hattler, B. G. and Federspiel, W. J., "A Mathematical Model of Gas Exchange in an Intravenous Membrane Oxygenator," *Ann. Biomed. Eng.*, **26**, 166 (1998).
- Ichiba, S. and Bartlett, R. H., "Current Status of Extracorporeal Membrane Oxygenation for Severe Respiratory Failure," *Artificial Organs*, **20**, 120 (1996).
- ISO/DIS 7199 International Standard: Cardiovascular Implantants and Artificial Organs-Blood-Gas Exchangers (1996).
- Kim, G. B., Kwon, T. K., Jheong, G. R. and Lee, S. C., "Gas Transfer and Hemolysis Characteristics of a New Type Intravenous Lung Assist Device," *J. Biom. Eng. Res.*, **24**(2), 121 (2003).
- Lee, S. C. and Kim, K. B., "Liquid Flow and Pressure Drop of an Outside Flow Membrane Oxygenator with Hollow Fibers," *J. Biomed. Eng. Res.*, **23**(1), 27 (2002).
- Morin, P. J., Gosselin, C., Picard, R., Vincent, M., Giundoin, R. and Nicholl, C. I. H., "Implantable Artificial Lung," *J. Thorac. Cardiovasc. Surg.*, **74**, 130 (1977).
- Mortensen, J. D., "Intravascular Oxygenator: A New Alternative Method for Augmenting Blood Gas Transfer in Patient with Acute Respiratory Failure," *Artif. Organs*, **16**, 75 (1992).
- Mulder, M., *Basic Principles of Membrane Technology*, AA Dordrecht, Kluwer Academic Publishers, Netherlands, 418 (1996).
- Naito, K., Mizuguchi, K. and Nosè, Y., "The Need for Standardizing the Index of Hemolysis," *Artificial Organs*, **18**, 7 (1994).
- Nguyen, T. T., Zwischenberger, J. B., Tao, W., Traber, D. I., Herndon, D. N., Duncan, C. C., Bush, P. and Bidani, A., "Significant Enhancement of Carbon Dioxide Removal by a New Prototype IVOX," *ASAIO J.*, **39**, M719 (1993).
- Nosè, Y., *Recommended Practice for Assessment of Hemolysis in Continuous Flow Blood Pump*, West Conshohocken, PA: American Society of Testing and Materials, F04:40-41 (1998).
- Pesenti, A., Gattinoni, L., Kobolow, T. and Damia, G., "Extracorporeal Circulation in Adult Respiratory Failure," *ASAIO Trans.*, **34**, 43 (1988).
- Snider, M. T., Campbell, D. B., Kofke, W. A., High, K. M., Russell, G. B., Keamy, M. F. and Williams, D. R., "Venovenous Perfusion of Adult and Children with Severe Acute Respiratory Distress Syndrome," *ASAIO Trans.*, **34**, 1014 (1988).
- Snider, M. T., "Clinical Trails of an Intravenous Oxygenator in Patients with Adult Respiratory Distress Syndrome," *Anesthesiology*, **77**, 855 (1972).
- Streeter, V. L., Wylie, E. B. and Bedford, K., *Fluid Mechanics* (9th ed.), New York, McGraw-Hill Inc. (1998).
- Tanishita, K., Richardson, P. D. and Galletti, P. M., "Tightly Wound Coils of Microporous Tubing: Progress with Secondary Flow Blood Oxygenator Design," *Trans. ASME*, **21**, 216 (1975).
- Vaslef, S. N., Mockros, L. F., Anderson, R. W. and Leonard, R. J., "Use of a Mathematical Model to Predict Oxygen Transfer Rates in Hollow Fiber Membrane Oxygenators," *ASAIO J.*, **40**, 990 (1994).
- Weinberger, S. E., *Principles of Pulmonary Medicine*, Philadelphia: Saunders (1992).
- Weissman, H. M. and Mockros, L. F., "Gas Transfer to Blood Flowing in Coiled Circular Tubes," *J. Eng. Mech. Div. ASCE*, **94**, 857 (1968).
- Woodhead, M. A., "Management of Pneumonia," *Respir. Med.*, **86**, 459 (1992).